International Journal of Engineering and Technical Research (IJETR)
ISSN: 2321-0869 (O) 2454-4698 (P), Volume-14, Issue-1, January-June 2024

# Behavior of the parameters of an overhead transmission line non-uniform with frequency variations

**Gustavo Rafael de Souza Reis, Willian Marlon Ferreira**

***Abstract*— Generally, electrical energy transmission towers have different configurations due to the reliefs where they are installed. This requires the use of different types of configurations and structures, which can make an electrical network very complex. This article presents the influence of transmission tower profiles for overhead lines. To analyze the behavior of the lines, the JMarti model was used. The influence of frequency on the transmission line parameters is also demonstrated, which highlights the dependence and relationship between these quantities.**

***Index Terms*— Configurations, frequency, transmission line, reliefs.**

## I. Introduction

In the analysis of electromagnetic transient phenomena, it is already known that the resistance and inductance of transmission lines per unit length are frequency dependent due to the skin effect and earth return currents in the soil [1], [2]. Electromagnetic transient calculations are usually carried out assuming that transmission lines are uniform, i.e. with constant cross-section and constant electrical properties of conductors and dielectrics.

However, there are cases in which the electrical parameters of a transmission line have relevant variations along its length, and disregarding such variations may produce results that are inappropriate for the line's behavior.

As an example, we can mention the different configurations of the towers, arrangement of conductors, relief and electrical characteristics of the ground. The set of these variations characterizes a non-uniform transmission line.

For analysis of transmission line parameters, several models have been proposed to include the frequency dependence of line parameters [2], [3] in order to adequately characterize their behavior.

A non-uniform line can be modeled in computer programs [4], dividing the line into several uniform segments.

Another widely used method is the lumped parameter model that represents the distributed nature of line parameters by grouping them into segments called π equivalents. To accurately represent the distributed nature of the parameters for a given frequency, the line must have a sufficiently high number of segments, which makes the model unfeasible in practice. Furthermore, a single frequency should be adopted in the analysis, rather than a broad spectrum. The use of the spectrum makes it possible to verify the behavior of the transmission line at higher frequencies. Therefore, this model has limitations for these studies. However, this model has been used to analyze slow transient responses, such as short circuits and switching.

On the other hand, one of the most used and widely disseminated models is JMarti [2]. This model was developed and has been a great contribution in the studies and development of a transmission line model in the time domain. The model uses recursive convolutions, fitting techniques, and the characteristic method to solve the transmission line equations. As a result, it has proven to be a suitable and reliable model for power grid simulations at high frequencies. Furthermore, due to its simplicity in formulation, it was incorporated into offline simulation software [3].

In this work, a medium transmission line was considered, segmented into three parts, with each segment having specific characteristics of length, tower height, arrangement of conductors and electrical resistivity of the soil. As a result, a non-uniform line was obtained, where the influence of the variation of these characteristics in relation to their electrical parameters was evaluated.

## II. Electrical Network Analyzed

The electrical network considered is a single-phase overhead transmission line 150 km long, with one conductor per phase, with voltage 230 kV (1 pu), and load of 1500 Ω. The electrical conductors are made of aluminum, with an external radius of 4.68 mm, whose electrical conductivity is approximately 3.8 x $10^7$ S/m.

The Fig. 1 illustrates the line divided into three segments, where $C_i$ corresponds to the configuration of the respective segment.

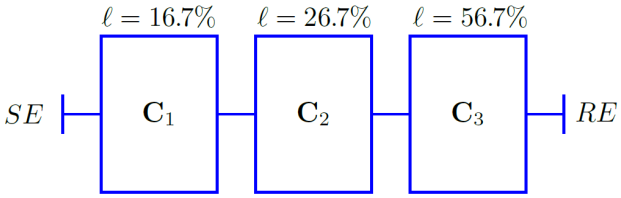


*Figure 1 – Segmented transmission line with three configurations.*

The sending terminal (*SE*) and the receiving terminal (*RE*) are located at the ends of the transmission line.

The Table I presents other information about the configuration.

**Gustavo Rafael de Souza Reis**, Electrical Engineering, Federal Institute of Minas Gerais (IFMG), Ipatinga, Brazil, (e-mail: gustavo.reis@ifmg.edu.br).

**Willian Marlon Ferreira**, Electrical Engineering, Federal Institute of Minas Gerais (IFMG), Ipatinga, Brazil, (e-mail: willian.ferreira@ifmg.edu.br).

TABLE I
LINE SEGMENTS AND THEIR RESPECTIVE CONFIGURATIONS.

| Greatness | $C_1$ | $C_2$ | $C_3$ | $C_T$ |
|---|---|---|---|---|
| Conductor height (meters) | 10 | 25 | 12 | 15.7 |
| Length (km) | 40 | 25 | 85 | 150 |
| Soil resistivity $\rho_g$ (Ω.m) | 30 | 400 | 1000 | 477 |

In the $C_T$ configuration, the height of the conductors and the soil resistivity were obtained by the simple arithmetic average of the three segments. The length of this configuration was considered the sum of the three segments $C_1$, $C_2$ and $C_3$.

## III. FREQUENCY DOMAIN ANALYSIS

The voltages at any point on the transmission line, in sinusoidal permanent regime, can be related by a matrix with characteristic and mutual impedances between phases:

$$\frac{d\tilde{V}(x)}{dx} = -\left[\tilde{R}' + j\omega\tilde{L}'\right]\tilde{I}(x) = -\tilde{Z}'(x)\tilde{I}(x) \tag{1}$$

where

$$\tilde{Z}'(\omega) = \tilde{Z}_i'(\omega) + \tilde{Z}_e'(\omega) + \tilde{Z}_g'(\omega) \tag{2}$$

$\tilde{Z}'$ is the matrix of longitudinal impedances per unit line length.

### A. *External longitudinal parameters*

Propagations in phase components have delays corresponding to the propagation speeds for the eigen and mutual terms of the propagation matrix, which are different in a generic line [5].

In the case of an ideal line, the conductor and the ground are assumed to be perfect conductors, and the characteristic impedances are called surge impedances.

Knowing that units $\tilde{Z}_e'(\omega) = j\omega\tilde{L}_e'$ can be defined $\tilde{L}_e'$, invariant with frequency, whose parameters are obtained with the following expressions:

$$\tilde{L}_e' = \frac{\mu_0}{2\pi} M \tag{3}$$

With the terms of matrix *M* given by:

$$m_{ii} = \ln\left(\frac{2h_i}{r_i}\right) \tag{4}$$

$$m_{ij} = \ln\left(\frac{D_{ij}}{d_{ij}}\right) \qquad (i \neq j) \tag{5}$$

onde *i* e *j* são índices dos elementos da matriz *M*.

### B. *Internal longitudinal parameters of cylindrical conductors*

The internal resistance and inductance matrices can be calculated using the following equations [6]. This is an improved approximation for calculating these parameters:

$$Z_i' = \sqrt{\left(R'_{i(cc)}\right)^2 + \left(Z'_{i(HF)}\right)^2} \tag{6}$$

where

$$R'_{i(cc)} = \frac{1}{\sigma\pi r_0^2} \tag{7}$$

$$Z'_{i(HF)} = \frac{1}{2\pi r_0}\sqrt{\frac{\mu}{\sigma}}\sqrt{j\omega} \tag{8}$$

### C. *Parameters associated with ground return*

For a soil with non-zero resistivity (finite conductivity) and a transmission line with *n + 1* conductors, the effect of the penetration of electric and magnetic fields in this medium can be accounted for through the impedance matrix associated with the return through the soil, given per:

$$\tilde{Z}'_g = \tilde{R}'_g + j\omega\tilde{L}'_g \tag{9}$$

The calculation of the return impedance matrix associated with the ground can be obtained by low frequency approximations [7]:

$$\tilde{Z}'_{gii} = \frac{j\omega\mu_0}{2\pi}\ln\left[\frac{h_i + \dot{p}}{h_i}\right] \tag{10}$$

$$\tilde{Z}'_{gij} = \frac{j\omega\mu_0}{2\pi}\ln\left[\frac{\sqrt{\left(h_i + h_j + 2\dot{p}\right)^2 + d_{ij}^2}}{\sqrt{\left(h_i + h_j\right)^2 + d_{ij}^2}}\right] \tag{11}$$

$$\dot{p} = \frac{\rho_g}{j\omega\mu_0} \tag{12}$$

where $\rho_g$ is the resistivity of the soil and $\dot{p}$ the complex depth.

### D. *Cross-sectional parameters*

In sinusoidal steady state, for a specific frequency, the following matrix relationship can be obtained for a transmission line with *n + 1* conductors:

$$\frac{d\tilde{I}(x)}{dx} = -\left[\tilde{G}' + j\omega\tilde{C}'\right]\tilde{V}(x) = -\tilde{Y}'(x)\tilde{V}(x) \tag{13}$$

Where

$$\tilde{Y}'(\omega) = \left[\tilde{Y}_e'^{-1}(\omega) + \tilde{Y}_g'^{-1}(\omega)\right]^{-1} \tag{14}$$

$\tilde{Y}'$ is the transverse admittance matrix per unit line length.

For a frequency spectrum of up to 10 MHz and soil resistivity of up to 1000 Ω.m, we arrive at:

$$\tilde{Y}'(\omega) = \tilde{Y}_e'(\omega) = j\omega\tilde{C}' \tag{15}$$

The capacitance matrix is obtained with the following expression [5]:

$$\tilde{C}' = 2\pi\varepsilon_0 M^{-1} \tag{16}$$

Alternatively, the matrix of capacitances per unit length can be calculated from the matrix of external inductances as:

$$\tilde{C}' = \pi\varepsilon_0 \tilde{L}'_e \tag{17}$$

*E. JMarti transmission line model*

The formulation of the JMarti model for power transmission lines in the time domain is based on the line equations in the frequency domain:

$$\begin{bmatrix} V_k(\omega) \\ I_k(\omega) \end{bmatrix} = \begin{bmatrix} \cosh(\gamma(\omega)\ell) & -Z_C(\omega)senh(\gamma(\omega)\ell) \\ -\dfrac{senh(\gamma(\omega)\ell)}{Z_C(\omega)} & -\cosh(\gamma(\omega)\ell) \end{bmatrix} \cdot \begin{bmatrix} V_m(\omega) \\ I_m(\omega) \end{bmatrix} \tag{18}$$

where $\ell$ is the length of the line, $\gamma(\omega)$ is the propagation constant and $Z_C$ is the characteristic impedance, define by:

$$Z_C(\omega) = \sqrt{\frac{R(\omega) + j\omega L(\omega)}{G + j\omega C}} \tag{19}$$

$$\gamma(\omega) = \sqrt{|R(\omega) + j\omega L(\omega)| \cdot (G + j\omega C)} \tag{20}$$

Changing the variables in equation (18),

$$\begin{bmatrix} F_k(\omega) \\ B_k(\omega) \end{bmatrix} = W \begin{bmatrix} V_k(\omega) \\ I_k(\omega) \end{bmatrix} \tag{21}$$

$$\begin{bmatrix} F_m(\omega) \\ B_m(\omega) \end{bmatrix} = W \begin{bmatrix} V_m(\omega) \\ I_m(\omega) \end{bmatrix} \tag{22}$$

$$\begin{bmatrix} F_k(\omega) \\ B_k(\omega) \end{bmatrix} = W \begin{bmatrix} \cosh(\gamma(\omega)\ell) & -Z_C(\omega)senh(\gamma(\omega)\ell) \\ -\dfrac{senh(\gamma(\omega)\ell)}{Z_C(\omega)} & -\cosh(\gamma(\omega)\ell) \end{bmatrix} \cdot W^{-1} \begin{bmatrix} F_m(\omega) \\ B_m(\omega) \end{bmatrix} \tag{23}$$

where

$$W = \begin{bmatrix} 1 & Z_C(\omega) \\ 1 & Z_C(\omega) \end{bmatrix} \cdot \begin{bmatrix} V_m(\omega) \\ I_m(\omega) \end{bmatrix} \tag{24}$$

$$\begin{bmatrix} F_k(\omega) \\ B_k(\omega) \end{bmatrix} = W \begin{bmatrix} 0 & e^{\gamma(\omega)\ell} \\ e^{-\gamma(\omega)\ell} & 0 \end{bmatrix} \cdot \begin{bmatrix} F_m(\omega) \\ B_m(\omega) \end{bmatrix} \tag{25}$$

being used to introduce forward and backward scrolling functions.

Fig. 2 represents the resulting line model in the frequency domain.

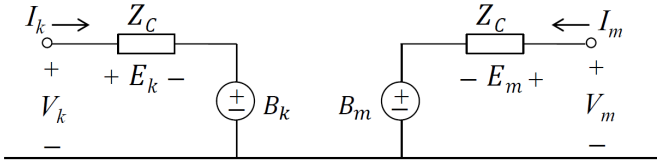


*Figure 2 – JMarti line model.*

## IV. IMPLEMENTATION IN ATP/EMTP.

The simulation was implemented in ATPDraw®. The segmented line is powered by a direct voltage source, as shown in Fig. 3.

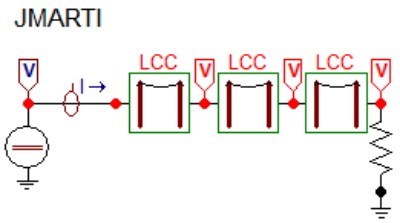


*Figure 3 – Segmented transmission line ($C_1$, $C_2$ and $C_3$).*

Fig. 4 illustrates the voltage behavior in each segment of the transmission line.

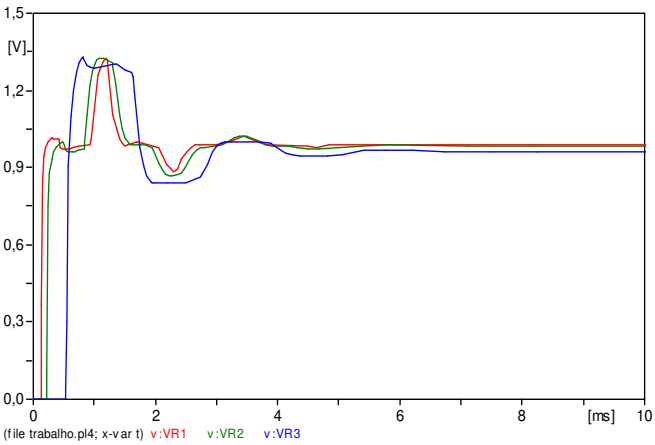


*Figure 4 – Voltage signal in each line segment ($C_1$, $C_2$ and $C_3$).*

It is observed that there is a variation in the voltage profile for each configuration, in addition to the smoothing of the wave due to the attenuation of the signal in the initial phase of the transient regime.

Fig. 5 illustrates the $C_T$ (single tower profile) configuration of the implemented transmission line.

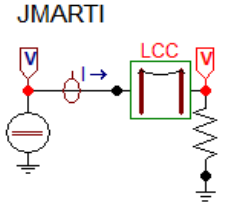


*Figure 5 – Transmission line $C_T$ configuration.*

The voltages at the receiver terminals for the segmented line ($C_1$, $C_2$ and $C_3$) and for the $C_T$ configuration are shown in Fig. 6.

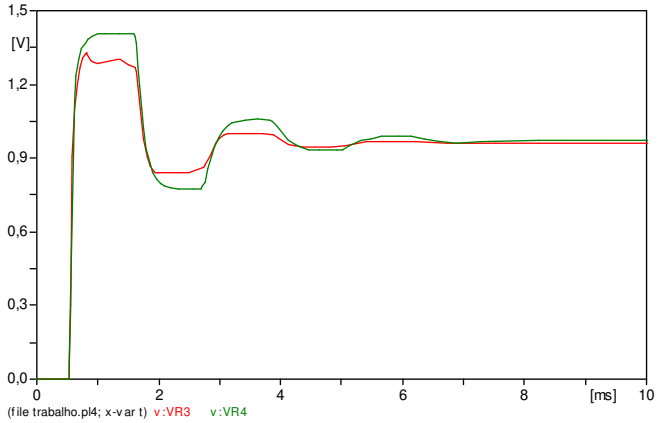


*Figure 6 – Comparison between voltages at the receiving terminals.*

The $C_T$ configuration does not adequately present the voltage behavior in the transient regime. Due to a single line configuration, it becomes a simplification that configures errors in the model, such as overvoltage. On the other hand, in the segmented line, the direct influence of segmentation on the voltage signal is perceived, not only in the initial moments of the transient, but also throughout the signal.

Fig. 7 compares the currents.

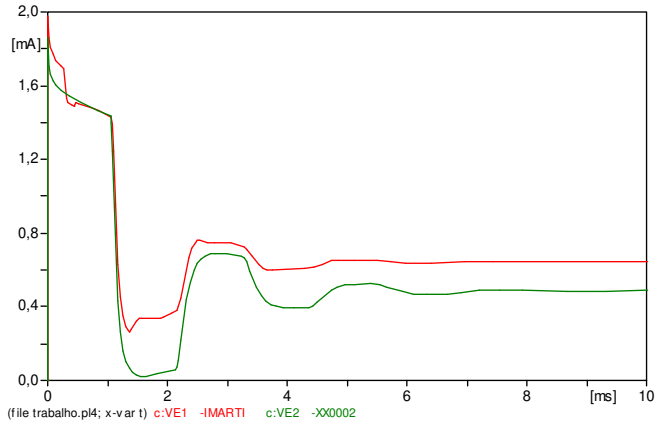


*Figure 7 – Comparison between currents.*

It can also be seen in the current signal that, depending on the configuration adopted, different behaviors occur for each situation. The peak current is lower in the $C_T$ configuration than for the segmented line ($C_1$, $C_2$ and $C_3$). Furthermore, there is a big difference in the entire signal. In sinusoidal steady state, the $C_T$ configuration does not reach the current value of the segmented line, which demonstrates a fragility of this type of approach. Current measurement values that do not correspond to the behavior of the line can cause damage to the electrical system, since it is not possible to measure such current in the event of a defect or failure.

To verify the influence of frequency on the transmission line parameters, a three-phase line was adopted with the same configurations of conductor height, line length and soil resistivity, reported in Table I. In this way, the configurations illustrated in Fig. 8 with the insertion of the distance between the conductors.

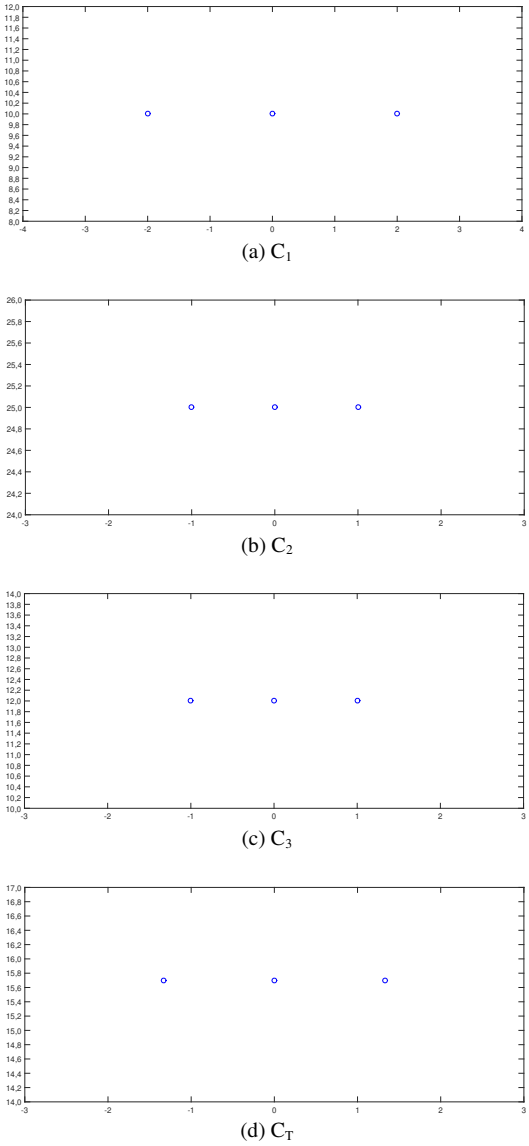

(a) $C_1$

(b) $C_2$

(c) $C_3$

(d) $C_T$

*Figure 8 – Arrangement of conductors for each segment.*

In the three-phase line, the behavior of the quantities from the phase 1 conductor was analyzed.

Fig. 9 demonstrates the variation in internal resistance against frequency variation.

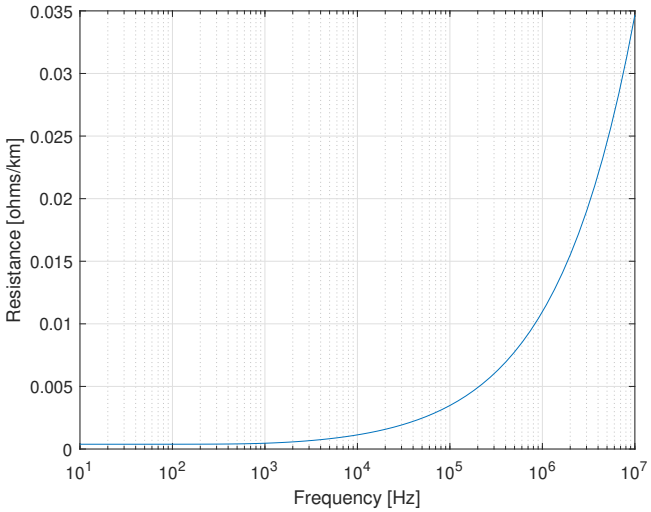


*Figure 9 – Internal resistance of the conductor versus frequency.*

Fig. 10 illustrates the variation in resistance associated with return through the ground with frequency variation.

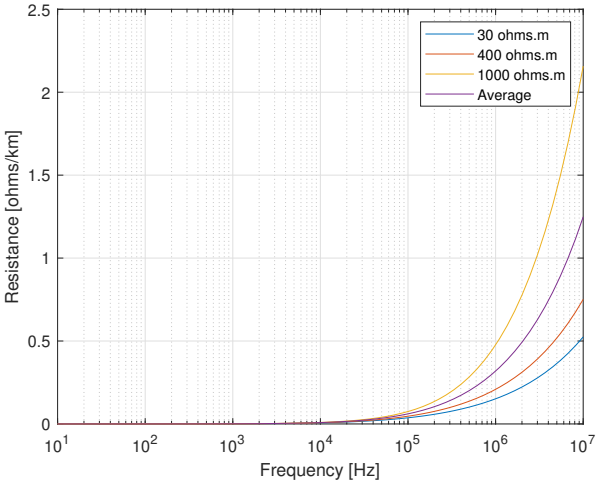


*Figure 10 – Resistance associated with soil return versus frequency.*

Fig. 11 illustrates the variation in resistance associated with return through the ground with frequency variation.

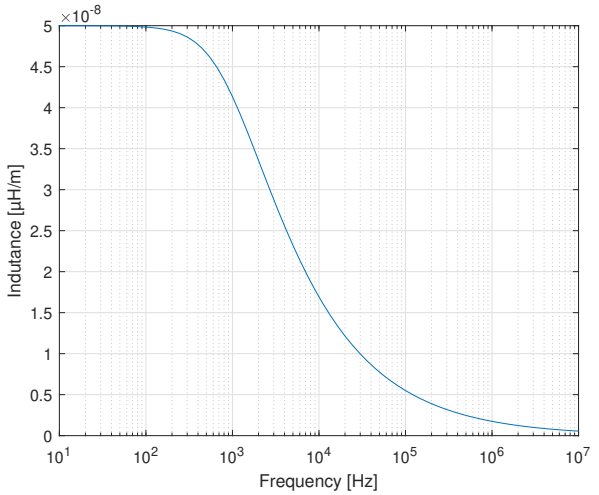


*Figure 11 – Internal inductance versus frequency.*

Fig. 12 illustrates the variation in resistance associated with return through the ground with variation in frequency.

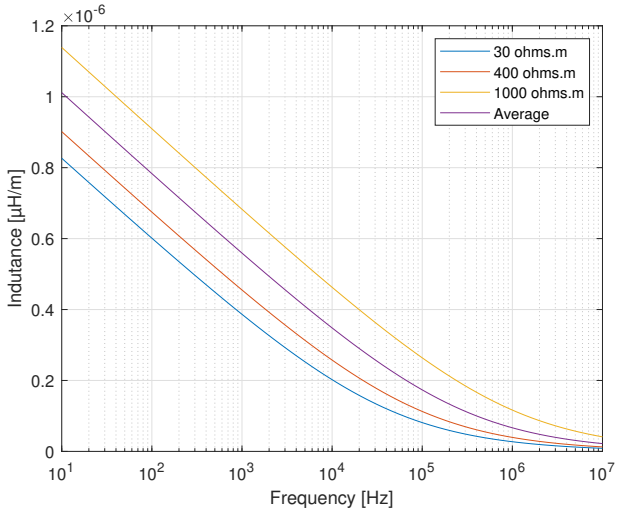


*Figure 12 – Inductance associated with ground return versus frequency.*

Through the illustrations presented, it can be seen that, in general, as the frequency increases, so does the resistance. In the conductor, there is a density of circulating electric current on its periphery, and in the center of the conductor this current tends to zero. This phenomenon is called the skin effect. Regarding the resistance associated with return through the soil, it was found that the resistance has higher values for soil with greater resistivity. Soils with high resistivities are more easily penetrated by the magnetic field, thus inducing greater currents associated with the soil.

On the other hand, when it comes to inductance, the higher the frequency, the lower its value due to the decrease in penetration depth. It can be seen that the inductance associated with the return through the ground is greater at high frequencies, since the electric field penetrates more easily, which consequently results in greater inductance.

## V. Conclusions

This paper investigated the influence of different types of tower configurations on an overhead single-phase transmission line. Changes in tower profiles cause very different behavior compared to a single configuration to represent the same line.

Furthermore, the behavior of the parameters of a three-phase transmission line in relation to frequency variation was also investigated. The answers presented demonstrated agreement with those found in the literature, demonstrating the validation of the implementations carried out.

## References

[1] J. R. Carson, “Wave propagation in overhead wires with ground return,” Bell system technical journal, vol. 5, no. 4, pp. 539–554, 1926.

[2] J. R. Marti, “Accurate Modeling of Frequency-Dependent Transmission Lines in Electromagnetic Transient Simulations,” IEEE Transactions on Power Apparatus Systems, vol. PAS-101, no. 1, pp. 147–157, 1982.

[3] T. Noda, N. Nagaoka, and A. Ametani, “Phase Domain Modeling of Frequency-Dependent Transmission Lines by Means of an ARMA Model,” IEEE Trans. on Power Delivery, vol. 11, no. 1, pp. 401–411, 1996.

[4] ATPDraw Windows version 6.0 p7. 1994-2015.

[5] L. C. Zanetta Júnior, “Transitórios eletromagnéticos em sistemas de potência”, Edusp, São Paulo, 2003.

[6] D. R. Holt and N. S. Nahman, “Coaxial-Line Pulse-Response Error Due to a Planar Skin-Effect Approximation,” IEEE Trans. Instrum. Meas., vol. 21, no. 4, pp. 515–519, 1972.

[7] Deri, A.; Tevan, G.; Semlyen, A.; Castanheira, A., “The Complex Ground Return Plane, a Simplified Model for Homogeneous and Multi-layer Earth Return,” IEEE Trans. PAS, vol. 100, no. 8, pp.: 3686-3693, 1981.